

Numerical Studies of the Compressible Ising Spin Glass

Adam H. Marshall and Sidney R. Nagel

The James Franck Institute and Department of Physics, University of Chicago, Chicago, Illinois 60637

Bulbul Chakraborty

The Martin Fisher School of Physics, Brandeis University, Waltham, Massachusetts 02454

(Dated: February 2, 2008)

We study a two-dimensional compressible Ising spin glass at constant volume. The spin interactions are coupled to the distance between neighboring particles in the Edwards-Anderson model with $\pm J$ interactions. We find that the energy of a given spin configuration is shifted from its incompressible value, E_0 , by an amount quadratic in E_0 and proportional to the coupling strength. We then construct a simple model expressed only in terms of spin variables that predicts the existence of a critical value of the coupling above which the spin-glass transition disappears.

PACS numbers: 75.10.Nr, 75.40.Mg, 05.50.+q

Lattice compressibility affects the nature of phase transitions in a variety of spin systems. The 2-dimensional (2-D) triangular Ising antiferromagnet, for example, is fully frustrated and shows no transition to an ordered state; however, when compressibility is added, this system exhibits a first-order transition to a striped phase [1, 2]. In the (unfrustrated) Ising ferromagnet, the introduction of compressibility changes the transition from second- to first-order so that the onset of nonzero net magnetization is simultaneous with a discontinuous change in the volume [3, 4]. Frustration is central to the nature of the spin-glass transition as it leads to large ground-state degeneracies [5, 6, 7, 8]. Because different states with the same spin-glass energy can couple differently to local lattice deformations, compressibility lifts the ground-state degeneracy and may dramatically alter the nature of the transition and the low-temperature spin-glass phase. Since magneto-elastic effects are always present to some degree in physical systems, their inclusion in spin-glass models may help explain some of the outstanding puzzles in spin-glass experiments [9]. We report here the effect of compressibility on a 2-D spin glass in which the lattice is allowed to distort locally while the entire system is held at constant volume.

The ground states of the previously studied compressible systems were always states that had already been ground states of those same systems without lattice distortion. In contrast, we find that as the coupling between magnetic interactions and lattice distortions is increased, the constant-volume compressible spin glass prefers spin configurations which had previously been excited states. We further find that the critical region just above the spin-glass temperature is suppressed as the coupling to lattice distortions increases so that above a certain value of the coupling, the spin-glass transition is eliminated entirely.

We study compressible two-dimensional Ising spin glasses on square lattices with periodic boundary con-

ditions at constant volume. The Hamiltonian is

$$\mathcal{H} = - \sum_{\langle i,j \rangle} J_{ij} S_i S_j + \alpha \sum_{\langle i,j \rangle} J_{ij} S_i S_j (r_{ij} - r_0) + U_{\text{lattice}}. \quad (1)$$

The first term is the energy of the standard (incompressible) Edwards-Anderson spin glass, with a sum over nearest neighbors. The spins S_i take the values ± 1 , and $J_{ij} \in \{\pm J\}$. The second term couples the spin interactions to local lattice distortions; r_{ij} is the distance between particles i and j , and r_0 is the particle separation of the undistorted lattice. We consider the coupling to linear order with coupling constant α . This term allows particles to move based on their magnetic interactions with their neighbors: a satisfied interaction (i.e. $J_{ij} S_i S_j = +1$) is enhanced when the particles move closer together, and an unsatisfied interaction is mitigated when the particles move apart. Because the distortions cannot be independent, the energy of a given configuration will depend on the local arrangement of satisfied (short) and unsatisfied (long) bonds, thus breaking the degeneracy inherent to the incompressible model.

The final term in the Hamiltonian represents the energy of the lattice itself: Hooke's-law springs of uniform spring constant k connect neighboring particles; springs are also required between next-nearest neighbors (across the diagonals of the squares) to prevent shear. All springs have their unstretched length equal to the natural spacing of particles on the undistorted lattice.

We identify two important parameters: $\bar{\delta} = J\alpha/k$ is a length scale which determines the typical size of the distortions from the uncompressed locations; the dimensionless quantity $\mu = J\alpha^2/k$ gives the average energy of the distortions relative to the original spin-glass energy. In our simulations, the parameters are chosen such that $\bar{\delta}$ is held fixed at $r_0/10$ while μ varies over the range of interest. The magnetic interaction strength J , which we set to unity, sets the overall energy scale.

We prepare a series of spin states and relax the lattice to its minimum potential energy via conjugant-gradient

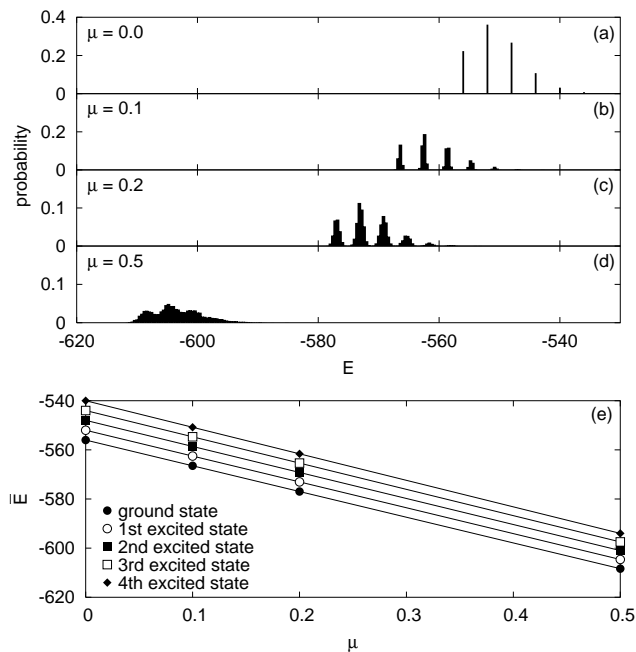


FIG. 1: (a) The energy spectrum of the incompressible spin glass consists of a series of delta functions separated in energy by $4J$. (b)–(d) As μ increases from zero, the spectrum shifts downward in energy, and each level spreads into a Gaussian-shaped band. The number of states under each curve remains constant. These data are from a single $L = 20$ realization at $T = 0.65$. (e) The average of each band is linear in μ ; the lines associated with different bands have slightly different slopes.

minimization [10]. These states are generated using standard Monte Carlo techniques on the incompressible spin-glass Hamiltonian. For $L = 3, 4, 5$, we enumerate all 2^{L^2} spin states for each bond realization. For larger systems, we acquire data from the ground state up to the highest-entropy states (where the spin energy is approximately zero) by running at multiple temperatures. We average over 100 different bond realizations.

As a function of the coupling, μ , and temperature, T , we examine the probability, $P(E)$, of finding a state with energy E . Typical results are shown in Fig. 1. For the uncoupled spin glass with $\mu = 0$, $P(E)$ is a series of delta functions separated by $4J$ [8] with heights proportional to $g(E)e^{-E/T}$, where $g(E)$ is the density of states (Fig. 1(a)). As μ increases, each initially degenerate level broadens and shifts to lower energy (Fig. 1(b)–(d)) by an amount proportional to μ (Fig. 1(e)).

As μ is increased, we calculate the energy shift of each configuration, $\Delta E \equiv E - E_0$, where E_0 is the energy of that configuration at $\mu = 0$. For each of the original levels (i.e., the δ -functions of Fig. 1(a)), we compute its average shift, $\overline{\Delta E}$, and width, σ . Both $\overline{\Delta E}$ and σ are quadratic in E_0 . The data for $\overline{\Delta E}$ can be scaled onto a common curve by dividing by L^2 , the number of particles

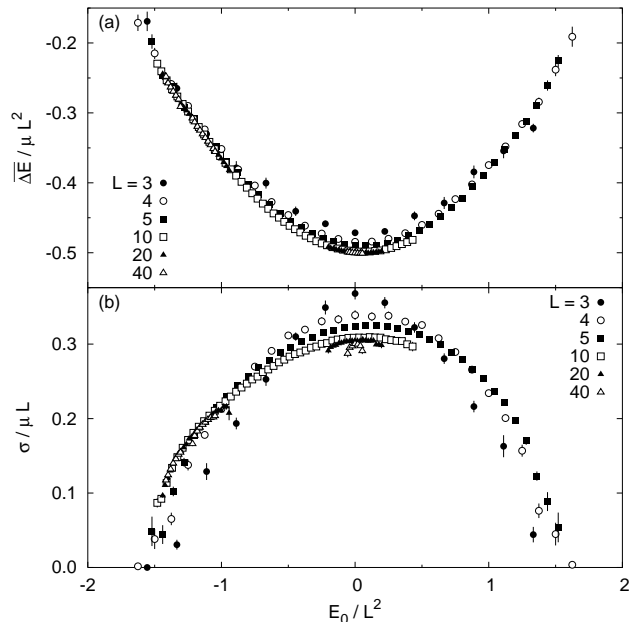


FIG. 2: (a) The average energy shift, $\overline{\Delta E} = \overline{E} - E_0$, divided by μ , plotted as a function of the initial energy; both axes have been scaled by the system size, L^2 . Data for different system sizes approach a common parabolic curve as L increases. (b) The scaled data for the width of each energy band also approach a common curve for large system sizes, but the scaling form indicates that the width is only linear in L . In the thermodynamic limit, the spread of each band is negligible compared to the average shift in energy.

(Fig. 2(a)):

$$\frac{\overline{\Delta E}}{\mu L^2} \sim -A + B \left(\frac{E_0}{L^2} \right)^2, \quad (2)$$

where $A = 0.50$ and $B = 0.13$. The smaller shift for low-energy states than for those near $E_0 = 0$ is to be expected since low-energy states, with many more satisfied than unsatisfied bonds, cannot distort as effectively as those with roughly equal numbers of each.

The data for the width of each band, σ , can be scaled onto a common curve by dividing by L (Fig. 2(b)):

$$\frac{\sigma}{\mu L} \sim C - D \left(\frac{E_0}{L^2} \right)^2, \quad (3)$$

where $C = 0.31$ and $D = 0.090$. While the energy shift is proportional to the area, the broadening is proportional only to the linear system size. In the infinite-size limit, the spreading of each level will be negligible relative to its energy shift. Eq. 3 also implies that the energy gaps between neighboring levels vanish when $\mu \approx 4/L$, i.e., for infinitesimal μ in the infinite-size limit. The previously discrete spectrum is thus rendered continuous.

The empirical form of Eq. 2 and the observation that the width of a level can be neglected in the thermodynamic limit suggest a simplified model. Because the shift

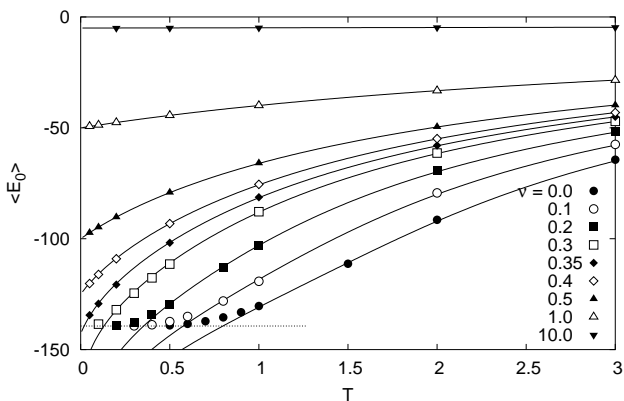


FIG. 3: Simulation results for $L = 10$ systems using the model of Eq. 4; solid lines indicate calculations using the entropy expression of Eq. 7. Below $\nu^* \approx 0.36$, the average bare spin energy approaches that of the ground state of the incompressible system (dotted line) as T is lowered. Above ν^* , however, the zero-temperature value of the average spin energy is given by Eq. 5. In this regime, the data may be predicted quite accurately.

of each level, $\overline{\Delta E}$, is simply proportional to E_0^2 , we replace the last two terms in the original Hamiltonian of Eq. 1 by a single term that gives that shift explicitly:

$$\mathcal{H}_{\text{approx}} = - \sum_{\langle i,j \rangle} J_{ij} S_i S_j + \frac{\nu}{L^2} \left(\sum_{\langle i,j \rangle} J_{ij} S_i S_j \right)^2. \quad (4)$$

Here we have absorbed multiplicative factors into the coupling constant $\nu \approx \mu/8$. The constant offset has been discarded as it does not affect the thermodynamics. The first term is again the standard Edwards-Anderson spin-glass energy. The second term is the resultant of the last two terms of Eq. 1: force balance provides a typical distortion that depends upon the total spin energy, and this distortion then substitutes into the coupling term, supplying another factor of the spin energy. This Hamiltonian contains only spin degrees of freedom, with four-spin, infinite-ranged interactions. The long-range nature of this model reflects the network of interconnected springs in the original compressible model.

The simplified model can be simulated directly and studied analytically. A straightforward derivation predicts a critical value of ν at which a zero-temperature transition takes place. From the approximate Hamiltonian of Eq. 4, the energy is $E = E_0 + \frac{\nu}{L^2} E_0^2$ (note that because the energy $E_0 \simeq L^2$ the last term does not vanish as L goes to infinity). The minimum of this function with respect to E_0 gives the level with lowest total energy and depends on ν according to

$$E_{0,\text{min}} = \frac{-L^2}{2\nu}. \quad (5)$$

For small ν , this minimum lies in the non-physical range

below the ground state $E_{0,\text{ground}}$. However, when

$$\nu = \frac{-L^2}{2E_{0,\text{ground}}} \equiv \nu^*, \quad (6)$$

the first excited state and the ground state of the incompressible system have the same energy. For large L , the ground state energy per spin, $E_{0,\text{ground}}/L^2$ has been determined to be approximately -1.4 [11]; thus, $\nu^* \approx 0.36$.

Above this value, ground states of the uncoupled system are no longer the lowest-energy states of the coupled system. This is seen in simulations of the simplified model (Fig. 3). As T is lowered to zero, the thermally averaged value of E_0 approaches that of the original ground state when $\nu < \nu^*$ but approaches the value predicted by Eq. 5 above ν^* .

Because they involve only spin degrees of freedom, the calculations for this model are standard spin-glass Monte Carlo simulations using the energy function given in Eq. 4. The presence of ν brings neighboring energy levels closer together in energy, and the large- ν simulations equilibrate rapidly. We find that the L -dependence of the simulations is somewhat trivial: when scaled by the number of particles, computed quantities converge quickly to asymptotic values as L increases [12].

The entropy of the $\pm J$ spin glass is well described by a quadratic with hyperbolic cosine corrections [12]:

$$S(E_0) = S_0 - S_1 E_0^2 - S_2 \cosh(S_3 E_0). \quad (7)$$

For $L = 10$, typical values are $S_1 = 2.5 \times 10^{-3}$, $S_2 = 8.1 \times 10^{-3}$, and $S_3 = 0.056$. Using this form, we minimize the free energy with respect to E_0 to obtain the average E_0 in the thermodynamic limit. The solution can be solved for numerically. Predicted values for E_0 as a function of T are shown as solid lines in Fig. 3; agreement with the data from finite-size systems is good for large temperatures and values of the coupling above ν^* . The breakdown of the prediction near the ground-state energy results from the lack of a low-energy cutoff in Eq. 7.

A transition occurs at ν^* . For larger values of ν , states of low total energy are also high-entropy states. Thus the competition between energy and entropy, on which the spin-glass transition depends, vanishes. An order parameter characterizing this new transition is the difference in spin energy of the level with lowest total energy and of the ground state of the uncoupled system, $E_{0,\text{min}} - E_{0,\text{ground}}$. Below ν^* , this quantity is zero; above, it increases as $\frac{1}{\nu^*} - \frac{1}{\nu}$, i.e. linearly in $\nu - \nu^*$ near the transition.

The temperature-reduced fluctuations of E_0 are shown versus T in Fig. 4(a) where the solid lines are calculations based on the entropy of Eq. 7. As ν increases, the maximum value of this quantity increases and shifts to lower T , and there appears to be a zero-temperature divergence that occurs as $\nu \rightarrow \nu^*$. This divergence in the fluctuations of the order parameter occurs due to the energy levels moving closer together, becoming equal at the

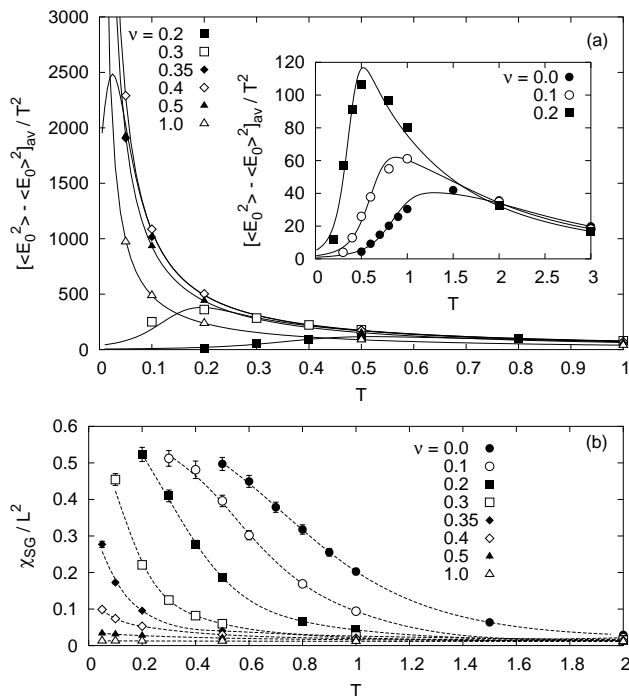


FIG. 4: (a) The temperature-reduced fluctuations in $\langle E_0 \rangle$ diverge as $T \rightarrow 0$ when $\nu > \nu^*$. Solid lines indicate the curves predicted from free-energy calculations. (b) The spin-glass susceptibility per spin, as a function of temperature. Dashed lines are merely guides to the eye. The sharp rise of χ_{SG} indicates the onset of critical behavior; the temperature at which this occurs is pushed down as ν increases until there is no longer a critical region. The spin-glass phase is thus eliminated.

critical value ν^* . The specific heat, which includes both energy terms in Eq. 4, shows no such behavior and always goes to zero as T is lowered.

The scaling behavior of the spin-glass susceptibility has been used to determine the temperature and critical exponents associated with the spin-glass transition [11, 13, 14]. Fig. 4(b) shows the spin-glass susceptibility per spin versus T for various values of ν . The increase of this susceptibility as T is lowered signals the onset of the critical phase that precedes the spin-glass transition [13]. As ν is increased, this critical phase shrinks, implying that the spin-glass transition is being destroyed.

In the T - ν plane, there exists an approximate boundary between the normal paramagnetic phase and the critical phase which signals the approach of spin-glass behavior. This boundary can be characterized, as a function of ν , by the temperature at which the temperature-scaled order-parameter fluctuations are maximized (see Fig. 4). It may also be approximated by the temperature at which

our predicted value of the average spin energy crosses the ground-state spin energy (see Fig. 3). In either case the phase boundary terminates at the same critical value ν^* .

We have limited our study to 2-dimensional systems. Preliminary results in 3-D indicate that $\overline{\Delta E}$ and σ also depend quadratically on E_0 with the same dependencies on the system size as were found in 2-D. This would suggest a similar result for how the spin-glass transition can be destroyed due to compressibility effects in 3-D. It is important to note that these results rely on the system being maintained at constant volume. We expect constant-pressure systems to behave differently since the low-energy levels should distort more effectively than higher-energy ones, in contrast to the constant-volume system. Finally, since the transition is not dependent upon the discrete nature of the energy spectrum, its presence is not limited to the $\pm J$ model but rather should be present in Gaussian models as well.

We thank S. Coppersmith, G. Grest, S. Jensen, J. Landry, N. Mueggenburg, and T. Witten for helpful discussions. BC acknowledges the hospitality of the James Franck Institute. SRN and AHM were supported by NSF DMR-0352777 and MRSEC DMR-0213745, and BC was supported by NSF DMR-0207106.

-
- [1] Z.-Y. Chen and M. Kardar, J. Phys. C **19**, 6825 (1986).
 - [2] L. Gu, B. Chakraborty, P. L. Garrido, M. Phani, and J. L. Lebowitz, Phys. Rev. B **53**, 11985 (1996).
 - [3] C. P. Bean and D. S. Rodbell, Phys. Rev. **126**, 104 (1962).
 - [4] D. J. Bergman and B. I. Halperin, Phys. Rev. B **13**, 2145 (1976).
 - [5] K. Binder and A. P. Young, Rev. Mod. Phys. **58**, 801 (1986).
 - [6] K. H. Fischer and J. A. Hertz, *Spin Glasses* (Cambridge University Press, 1993).
 - [7] M. Palassini and A. P. Young, Phys. Rev. B **63**, 140408 (2001).
 - [8] J. Lukic, A. Galluccio, E. Marinari, O. C. Martin, and G. Rinaldi, Phys. Rev. Lett. **92**, 117202 (2004).
 - [9] D. Bitko, N. Menon, S. R. Nagel, T. F. Rosenbaum, and G. Aeppli, Europhys. Lett. **33**, 489 (1996).
 - [10] W. H. Press, S. A. Teukolsky, W. T. Vetterling, and B. P. Flannery, *Numerical Recipes in C* (Cambridge University Press, 1997), 2nd ed.
 - [11] J.-S. Wang and R. H. Swendsen, Phys. Rev. B **38**, 4840 (1988).
 - [12] A. H. Marshall, in preparation.
 - [13] A. T. Ogielski, Phys. Rev. B **32**, 7384 (1985).
 - [14] R. N. Bhatt and A. P. Young, Phys. Rev. B **37**, 5606 (1988).